Influences of silicon carbide nanowires addition on IMC growth behavior of pure Sn solder during solid-liquid diffusion

Mulan Li
Jiangsu Normal University
Liang Zhang (zhangliang@jsnu.edu.cn)
Jiangsu Normal University https://orcid.org/0000-0003-3757-7009
Jiang Nan
Jiangsu Normal University
Sujuan Zhong
Zhengzhou Research Institute of Mechanical Engineering
Lei Zhang
Zhengzhou Research Institute of Mechanical Engineering

Research Article

Keywords: SiC nanowires, Sn solder, IMC growth, solid-liquid diffusion

Posted Date: March 25th, 2021

DOI: https://doi.org/10.21203/rs.3.rs-351790/v1

Influences of silicon carbide nanowires addition on IMC growth behavior of pure Sn solder during solid-liquid diffusion

Mu-lan Li [1], Liang Zhang [1, 2], Nan Jiang[1], Su-juan Zhong [2], Lei Zhang [2]

1 School of Mechatronic Engineering, Jiangsu Normal University, Xuzhou 221116, China;
2 State Key Laboratory of Advanced Brazing Filler Metals & Technology, Zhengzhou Research Institute of Mechanical Engineering, Zhengzhou 450001, China.

Abstract: In this paper, various mass fraction (0, 0.2, 0.4, 0.6, 0.8, 1.0 wt%) of silicon carbide nanowires (SiC) were incorporated into pure Sn solder to enhance the performances of Sn solder joint. The wetting behavior, shear strength and intermetallic compound (IMC) growth mechanism of Sn-*x*SiC/Cu solder during solid-liquid diffusion at 250 °C was investigated systematically. The experiment results demonstrated that the wettability of Sn-*x*SiC/Cu solder had a significant improvement when the addition of SiC was up to 0.6 wt%, and excessive additives would degrade the wettability of the composite solder. The formation of the Cu_6Sn_5 IMC layer was observed at the Sn-*x*SiC solder/Cu interface. Meanwhile, SiC as an additive was conducive to restraining the growth of interfacial IMC during soldering process and the IMC thickness overtly fell down after doping 0.8 wt% SiC into Sn solder. Moreover, SiC addition would contribute to enhancing the mechanical performance of Sn solder joint. The fracture mechanism of solder joint changed from a mix of brittle and ductile fracture to a characteristic of typical ductile fracture.

Keywords: SiC nanowires; Sn solder; IMC growth; solid-liquid diffusion

Correspondence: Liang Zhang, zhangliang@jsnu.edu.cn

1 Introduction

Sn-based solder, as a familiar material for the interconnection between substrates and parts of electron devices, provides for mechanical and electrical joints [1]. Solder joint is the product taken shape by the solder materials under the process of high temperature soldering, and its reliability is influenced by the formation of IMC at solder/substrate [2]. Due to the intrinsic brittleness of IMC, the joint strength will be degraded as the thickness of IMC layer increases remarkably, while thin IMC layer is conductive to improve the joint reliability with effect [3]. Numerous researches have been investigated the reaction at solder/substrate interface and the IMC growth kinetics of lead-free solder/substrate during soldering process [4]. Zhang et al.[5] pointed out that adding 0.5 wt% micro-sized CuZnAl particles into Sn58Bi put off the interfacial Cu_6Sn_5 and Cu_3Sn IMCs growth and decreased voids formation. The same results were observed in the interfacial surface of Cu/Sn58Bi/Cu [6]. As for the interface of Sn-3.8Ag-0.7Cu/Fe solder [7], CuZnAl particles could also hinder $FeSn_2$ IMC growth and reduce its thickness. Jiang et al. [8] stated that choosing 0.1 wt% Ti nanoparticles as additives suppressed the growth of Cu_6Sn_5 IMC at interfacial Sn58Bi/Cu solder during reflowing.

Considering the inherent toxicity of lead element which is hazardous to the environment and individual health, many countries have legislated against the use of lead in electronic packaging [9, 10]. So a range of lead-free Sn-based solders were selected as alternatives to Pb-containing solder, such as binary or ternary Sn-Bi, Sn-Cu, Sn-Ag-Cu solder etc [11-13]. Additionally, researchers usually selected micro/nano-metric materials as strengthened additives added into pure Sn solder to promote the reliability of solder joints, such as single metallic particles or elements (Ag, Bi, Cu, etc.) [14-16] and carbon-based materials [17]. Sun et al. [18] demonstrated that Cu atoms in Cu substrate could react with Sn atoms in Sn solder rapidly at high temperature and two different IMC layers of the typical Cu_6Sn_5 and Cu_3Sn were observed at the interface as the transient liquid phase bonding time increased. Meanwhile,

micrometric CuZnAl particles added to Sn solder could absorb on the surface of Sn atoms, prohibiting the Sn and Cu atoms from reacting and then refraining interfacial surface IMC layer growth of Cu/Sn-0.5CuZnAl/Cu. Also, there were studies [17, 19] that indicated that 0.075 wt% carbon nanotubes (CNTs) or 0.7 wt% Cu nanoparticles as strengthening phases introduced into Sn solder decreased the interfacial Cu_6Sn_5 IMC thickness mostly. Moreover, Ag_3Sn nanoparticles added to Sn solder could restrain the overgrowth of the interfacial Cu_6Sn_5 IMC in that it would be aggregated on IMC surface and prevent Sn and Cu ions from diffusing at the solder/substrate interface [14].

In this paper, SiC was chose to be a strengthening phase due to its excellent mechanical properties. Various mass fraction ranging from 0 wt% to 1.0 wt% of SiC powders were incorporated into pure Sn solder to fabricate Sn-*x*SiC composite solder. The growth behavior of Sn-Cu IMC between Sn-*x*SiC solder and Cu substrate after soldering at 250 °C was investigated. Additionally, the wettability and the shear resistance of Sn-*x*SiC composite solder were also discussed.

2 Experimental procedures

2.1 Materials preparation

Halogen-free lead-free flux was blend with micro-sized Sn powder in a solder paste mixer at a ratio of 3:20 in order to fabricate pure Sn solder paste as matrix materials. As shown in Fig.1, the morphology of SiC was exhibited, and the diameter of SiC was 20-200 nm while the length of it was 2-30 μm. The Sn-*x*SiC (x = 0, 0.2, 0.4, 0.6, 0.8, 1.0 wt%) composite solder pastes, with the SiC powder and pure Sn solder paste as the raw materials, were synthesized via mechanical stirring. Cu sheets sized of 25 mm×25 mm×0.20 mm, as the substrates, were selected to be washed with alcohol in an ultrasonic clearing machine for 2 min.

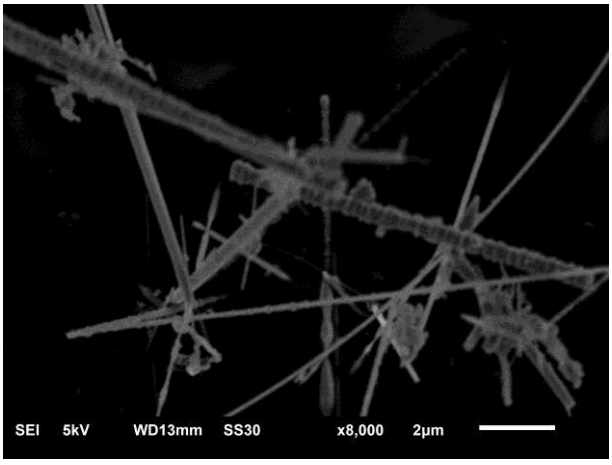

Fig.1 SEM image of SiC.

2.2 Wettability

As a rule, the wettability is characterized by the contact angle and spreading area [8]. In this experiment, wetting behavior was indicated by computing the spreading area. First of all, take 0.2 ± 0.001g of Sn-*x*SiC solder and place it on the center of Cu substrate respectively. Subsequently, the test specimens were heated by a graphite thermostatic heating plate at a peak temperature of 250 °C for 1 min and then move them away the heating plate when they were cooled to room temperature. Lastly, it is a necessity to take advantage of Image-J software to calculate the spreading areas three times, respectively, as to guarantee the accuracy of the test data.

2.3 Interfacial IMC layer growth

As for the kinetics of IMC layer growth at the interface of Sn-*x*SiC/Cu, the Sn-SiC samples were

imbedded in resin epoxy after cutting that along the cross section. After that the inlaid specimens were grinded with abrasive paper and polished with diamond grinding paste. Afterwards, the cross section was corroded with a mixed solution of 5% nitric acid and 95% alcohol for 4 seconds. Lastly, scanning electron microscope (SEM) was utilized to observe the interfacial IMC morphology. According to Eq.(1), the average thickness of interfacial IMC can be calculated:

$$\chi = \frac{A}{L} \tag{1}$$

where χ represents the mean thickness of IMC layer, A represents the IMC layer area, L represents the IMC layer length, as shown in Fig.2.

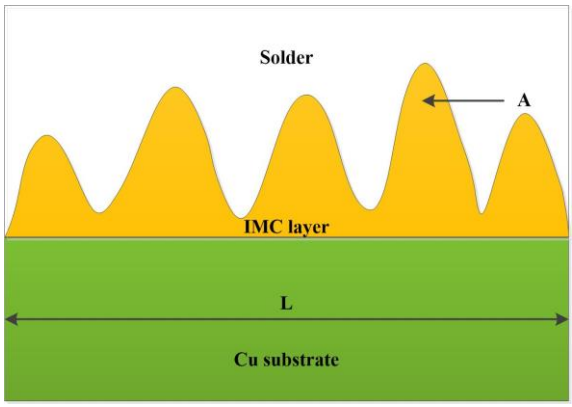

Fig.2 Diagrammatic drawing of interfacial IMC.

2.4 Mechanical property

For the shear experiment, the UTM5000 electronic universal testing machine, in a shear rate of 2mm/min, was employed to acquire the shear strength value. The size of Cu sheets was 40mm×4.0mm×0.6mm and the solder paste was about 0.50 mm in this test. The schematic diagram of shear test was obviously obtained in Fig.3. After the specimens conducted the soldering process, the shear test was made use of SEM to observe fracture morphology.

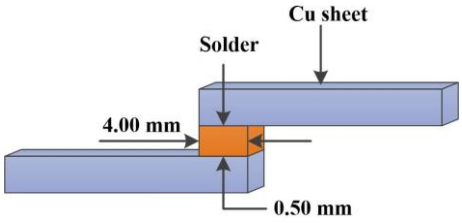

Fig.3 Diagrammatic drawing of shear test for Sn-*x*SiC solder.

3 Results and discussion

3.1 Wettability

As shown in Fig.4, the spreading areas of Sn-*x*SiC composite solder joints are obtained. What is vividly in the bar chart is that the wetting area firstly increases and then decreases with an increase of weight percentage of SiC. When the amount of SiC added to pure Sn solder is up to 0.6 wt%, the spreading area reaches 65.85 mm^2, with an increase of 27.49% as compared to the pure Sn solder. Nevertheless, the spreading area has a precipitous decline as the addition of SiC is over 0.6 wt%. The wettability improvement can be explained by the Young equation:

$$\cos\theta = \frac{\xi_{gs} - \xi_{ls}}{\xi_{gl}} \tag{2}$$

where θ refers to the wetting angle, ξ_{gl}, ξ_{gs} and ξ_{ls} refer to the interfacial tension of gas/fluid, gas/solid and fluid/solid, respectively. It is apparent that the smaller wetting angle means the larger spreading area, and the wettability of the solder performs better. Owing to the nanometric particles with high surface activity that tend to be absorbed on the solder surface, the surface tension of molten solder/substrate falls down and then the wettability of Sn solder containing SiC improves. Nevertheless, the excessive doping amount of SiC will appear agglomeration phenomenon in the solder matrix which contributes to a reduction of the viscosity of the Sn-SiC composite solder and then the wettability of the molten composite solder deteriorates. Thus, so important appropriate content of SiC addition to Sn solder is that contributes to promoting the wettability of the solder.

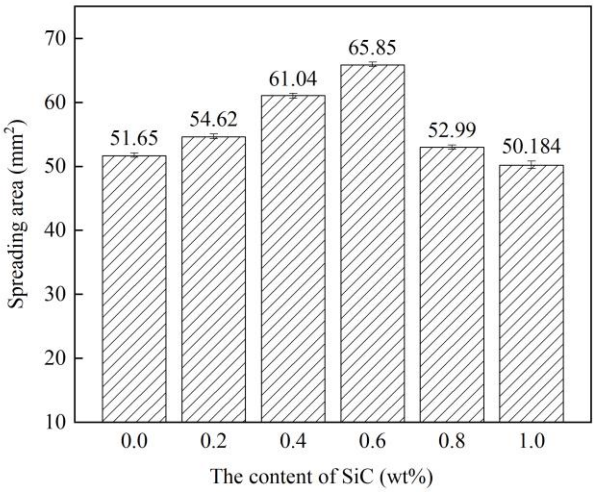

Fig.3 Column diagram of the spreading area varying with the addition content of SiC.

3.2 Interfacial IMC layer growth

Fig.4 exhibits the cross-sectional SEM image of Sn-*x*SiC/Cu interface after solid-liquid diffusion at 250 °C last for 1 min and the scallop-like IMC is formed at the interfacial Sn-*x*SiC/Cu solder joint after soldering. Through energy dispersive spectrometer (EDS) analysis as shown in Fig.5, it can be determined that the composition of IMC is Cu_6Sn_5 marked in Fig.4 (a). Cu_6Sn_5 IMC formation owes to the reaction of Sn element and Cu element diffusing from matrix and substrate, as described in Eq. (3):

$$6Cu + 5Sn \rightarrow Cu_6Sn_5 \quad (3)$$

It is obvious from Fig.4 that the SiC addition performs some function in reducing IMC thickness. Fig.6 exhibits the mean IMC thickness of Sn-*x*SiC/Cu solder measured by Image-J software. From Fig.6, it demonstrates that the IMC layer thickness of Sn-*x*SiC/Cu solder joint is less than that of the Sn/Cu solder joint, which reveals that adding SiC can suppress the IMC growth. Similar results were reported by Lee et al. [20] who stated that doping SiC could restrain the IMC growth at Sn58Bi solder/Cu interface with effect. As SiC addition increased, the IMC thickness at Sn-*x*SiC/Cu solder interface falls down. When the amount of SiC is up to 0.8 wt%, the Cu_6Sn_5 layer thickness has a maximum reduction, in which case, the thickness of IMC layer is reduced to 7.18 μm from 9.73 μm in pure Sn solder, with a decrease of 26.21%. On the one hand, the Cu_6Sn_5 layer gets thinner in that the SiC which nails at grain boundaries impedes the Sn and Cu atoms diffusion and then brings about the suppression of Cu_6Sn_5 growth. On the other hand, this can be attributed to the high surface energy of the nanoscale particles based on the adsorption theory, which can be described as following:

$$\sum_{\mathrm{K}} \gamma_C^{\mathrm{K}} \mathrm{A}_{\mathrm{K}} = \sum_{\mathrm{K}} \left(\gamma_0^{\mathrm{K}} - \mathrm{RT} \int_0^C \frac{\Gamma^{\mathrm{K}}}{C} \mathrm{d}C \right) \mathrm{A}_{\mathrm{K}} \tag{4}$$

where C is the concentration of SiC, A_{K} is the surface area of K plane, γ_C^{K} is the unit surface tension of the K plane containing SiC, γ_0^{K} is the unit surface tension of the K plane without SiC, T is the absolute temperature, R is the Planck constant, Γ^{K} is the adsorption capacity of SiC at K plane. When the adsorption capacity of SiC reaches the maximum as the mass fraction of nanoparticles added up to 0.8 wt%, the $\sum_{\mathrm{K}} \mathrm{A}_{\mathrm{K}} \int_0^C \frac{\Gamma^{\mathrm{K}}}{C} \mathrm{d}C$ reaches a maximum, which means the total surface energy of K plane is minimal according to Eq.(4). In this case, it can be concluded that appropriate SiC addition can inhibit the growth of interfacial IMC. But further adding SiC into Sn solder, the interfacial IMC thickness gets larger than that of the Sn-0.8SiC solder. Excessive addition will weaken the inhibition effect on IMC growth. It may ascribe that the excess SiC dopants are prone to be agglomerates so as to decrease their adsorption capacity, which will result in the weaken of the IMC inhibition.

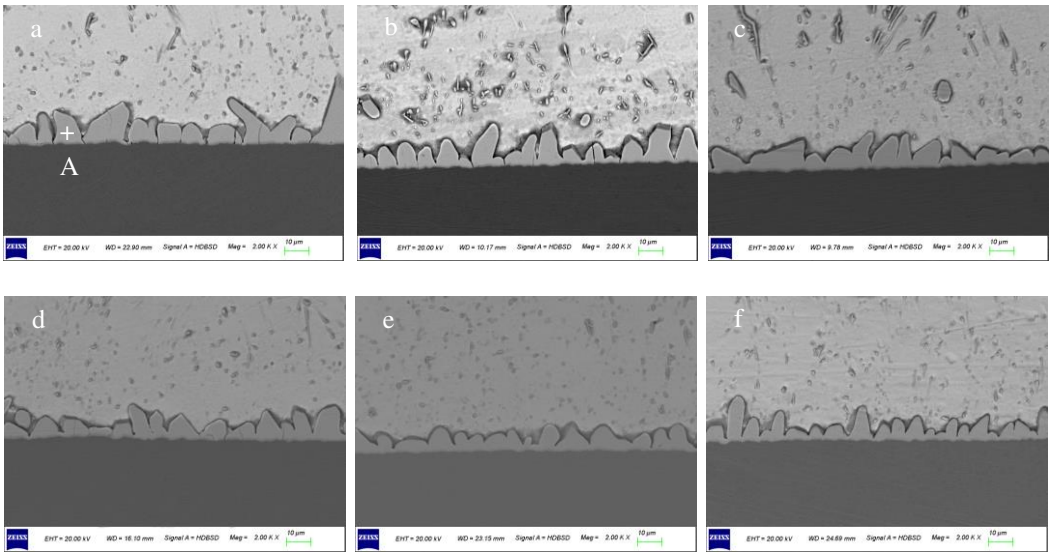

Fig.4 SEM morphology graph of the IMC at Sn-*x*SiC/Cu solder heated at 250 °C for 1 min: (a) *x*=0, (b) *x*=0.2, (c) *x*=0.4, (d) *x*=0.6, (e) *x*=0.8, (f) *x*=1.0.

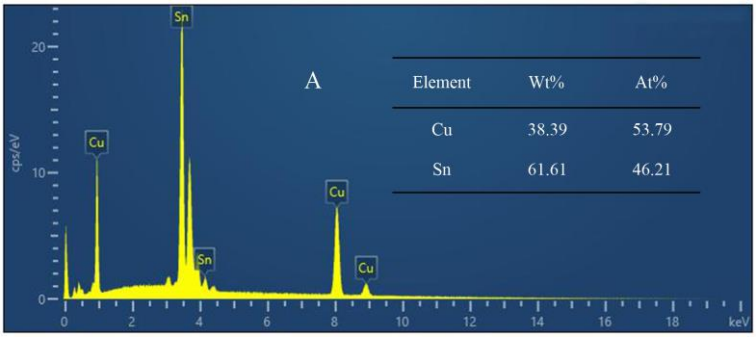

Fig.5 EDS analysis of IMC layer in Fig.4(a)

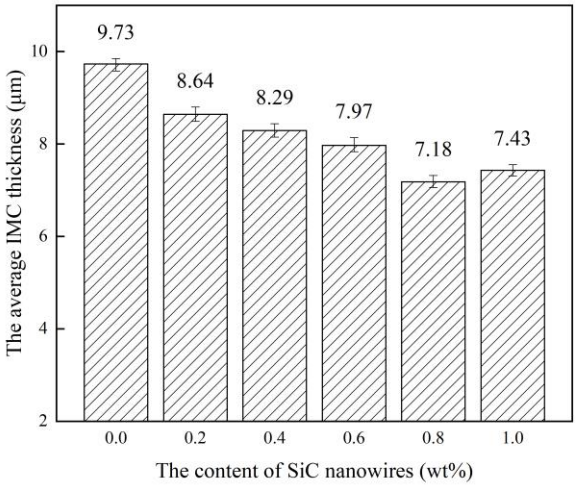

Fig.6 The average IMC thickness as different amount of SiC added to Sn solder.

3.3 Mechanical property

When it comes to the reliability of solder joint, the shear strength should be taken into account. As is shown in Fig.7, the shear strength varies with the mass fraction of SiC added into pure Sn solder. It can be conspicuously seen that doping SiC is conducive to strengthening the shear strength of pure Sn solder, an increase in the range of 0.977 MPa - 6.59 MPa. The shear strength puts on first and then falls down as the addition of SiC increased. When the amount of SiC added to Sn solder comes up to 0.8 wt%, the shear strength of Sn-SiC solder joint reaches a maximum value of 30.66 MPa from 24.07 MPa in pure Sn solder joint, an increase of 27.38%. The enhancement in mechanical performances of Sn-*x*SiC composite solder can be ascribed to dispersion strengthening and refinement strengthening mechanism. On one side, SiC dispersed in the solder matrix uniformly, tends to nail at IMC grain boundary and impede dislocation movement from generating. The dispersion strengthening can be clarified by the Orowan equation:

$$\sigma = \frac{2Gb}{\lambda} \tag{5}$$

where σ means the yield stress of the material, b means the Burger's vector of dislocation, G means shear modulus of the material and λ means the average grains spacing in the solder matrix. Doping SiC decreases the mean spacing of the dispersed grains, contributing to the enhanced mechanical performances in accordance with Eq. (5). On the other side, SiC added into Sn solder can exist as nucleation sites and then refine the microstructure of composite solder, resulting in the strengthened shear strength owing to the Hall-Petch relationship that can be expounded as following:

$$\sigma_y = \sigma_0 + \frac{K}{\sqrt{d}} \tag{6}$$

where σ_y equals to 0.2 times yield strength of material, d is the mean size of grains, σ_0 and K are material constants. What's more, the IMC layer connected with solder and substrate is characterized by brittleness [6], and therefore thicker IMC layer will degrade the bonding strength of solder joints. Meantime, the Sn-0.8SiC solder exhibits the thinner IMC thickness in comparison to pure Sn solder that is linked with the better bonding strength, significantly enhancing the mechanical performances of the composite solder joints, and then its shear strength is improved. In this condition, it is obvious that the shear strength gradually decreases when the content of SiC is over 0.8 wt%, which is concerned with the agglomeration phenomenon caused by adding powder too much brings about the increase of grain size and the

thickening of IMC layer.

The fracture morphologies of shear tested specimens are revealed in Fig.8. As shown in Fig.8 (b)-(f), after adding SiC into Sn solder, there are more dimples appearing in SEM morphology in comparison to Fig.8 (a). Meanwhile, the fracture mode of solder joint turns a brittle and ductile mixed mode to a ductile one, which is a reason that the shear strength of composite solder joint is superior than pure Sn solder joint. Among them, Fig.8 (e) exhibits the most dimples distributed in fracture surface and therefore the Sn-0.8SiC composite shows the best performance in the shear strength. Nonetheless, when the addition of SiC is excessive, the number of ductile dimples is decreased, giving rise to a reduction of shear strength. From what has been discussed above, we may safely come to a conclusion that the appropriate amount of SiC addition is 0.8 wt% in strengthening the mechanical performances of Sn-SiC composite solder greatly.

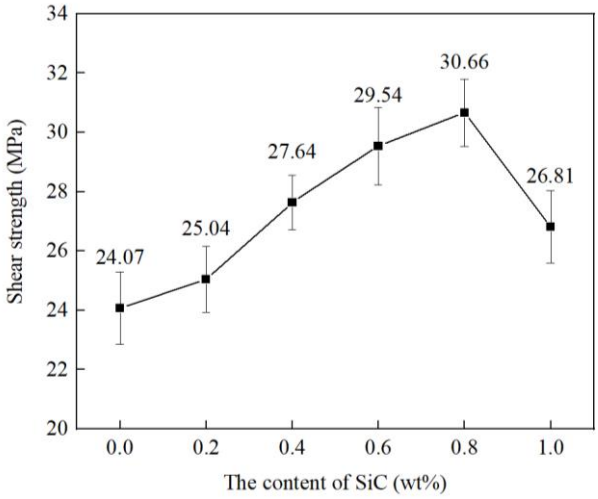

Fig.7 Curve graph of the shear strength as a function of SiC amount in Sn solder.

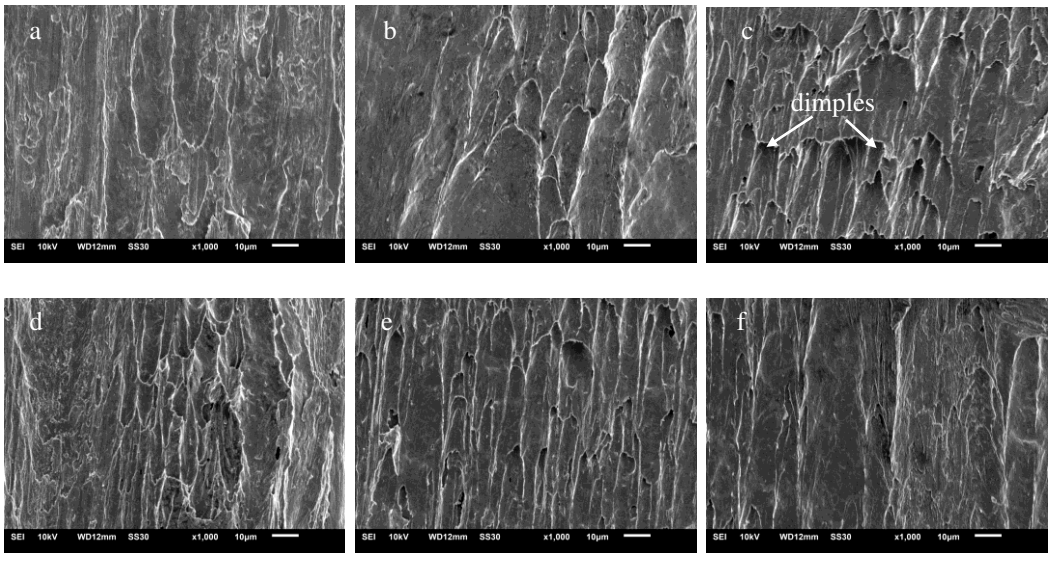

Fig.8 SEM graphs of fracture morphology of Sn-*x*SiC solder under tensile test: (a) $x = 0$, (b) $x = 0.2$, (c) $x = 0.4$, (d) $x = 0.6$, (e) $x = 0.8$, (f) $x = 1.0$.

4 Conclusions

In this study, the wettability, shear strength and the growth behavior of IMC of Sn-*x*SiC/Cu solder under solid-liquid diffusion at 250 °C were systematically investigated. The conclusions can be drawn as

following:

(1) The minor amount of SiC incorporated to Sn solder is conducive to enhancing the wettability of composite solder and the optimal content is 0.6 wt%.

(2) Adding 0.8 wt% SiC into pure Sn solder can impede the diffusion of Sn and Cu atoms, hindering the interfacial Cu_6Sn_5 IMC growth significantly.

(3) The SiC doping can effectively strengthen the shear strength of Sn-*x*SiC composite solder, and the fracture mode converts a brittle and ductile mode to a ductile mode after adding SiC into Sn solder.

Acknowledgements

The present work was under support of the Key project of State Key Laboratory of Advanced Welding and Joining (AWJ-19Z04), National Key Research and Development Project (2019YFF0217400), Central Plains science and technology innovation talent plan (ZYQR20180030).

References

[1] Tu K N, Liu Y X. Recent advances on kinetic analysis of solder joint reactions in 3D IC packaging technology[J]. Materials Science & Engineering, 2019, 136:1-12.

[2] Xiong M Y, Zhang L. Interface reaction and intermetallic compound growth behavior of Sn-Ag-Cu lead-free solder joints on different substrates in electronic packaging[J]. Journal of Materials Science, 2019, 54(2): 1741-1768.

[3] Tan A T, Tan A W, Yusof F. Influence of nanoparticle addition on the formation and growth of intermetallic compounds (IMCs) in Cu/Sn-Ag-Cu/Cu solder joint during different thermal conditions[J]. Science & Technology of Advanced Materials, 2015, 16(3):033505.

[4] Li M L, Zhang L, Jiang N, et al. Materials modification of the lead-free solders incorporated with micro/nano-sized particles: A review[J]. Materials &Design, 2021, 197:109224.

[5] Zhang L, Liu Z Q. Inhibition of intermetallic compounds growth at Sn-58Bi/Cu interface bearing CuZnAl memory particles (2-6 μm)[J]. Journal of Materials Science Materials in Electronics, 2020, 31(3):2466-2480.

[6] Xiong M Y, Zhang L, Sun L, et al. Effect of CuZnAl particles addition on microstructure of Cu/Sn58Bi/Cu TLP bonding solder joints[J]. Vacuum, 2019, 167:301-306.

[7] Zhang L, Long W M, Wang F J. Microstructures, interface reaction, and properties of Sn-Ag-Cu and Sn-Ag-Cu-0.5CuZnAl solders on Fe substrate[J]. Journal of Materials Science: Materials in Electronics, 2020, 31(9):6645-6653.

[8] Jiang N , Zhang L , Long W M , et al. Influence of doping Ti particles on intermetallic compounds growth at Sn58Bi/Cu interface during solid-liquid diffusion[J]. Journal of Materials Science: Materials in Electronics, 2021, 32:3341-3351.

[9] Chang S Y, Jain C C, Chuang T H, et al. Effect of addition of TiO_2 nanoparticles on the microstructure, microhardness and interfacial reactions of Sn3.5AgXCu solder[J]. Materials & Design, 2011, 32(10):4720-4727.

[10] Chellvarajoo S, Abdullah M Z. Microstructure and mechanical properties of Pb-free Sn-3.0Ag-0.5Cu solder pastes added with NiO nanoparticles after reflow soldering process[J]. Materials & Design, 2016, 90:499-507.

[11] Wang F J, Liu L T, Li D Y, et al. Electromigration behaviors in Sn-58Bi solder joints under different current densities and temperatures[J]. Journal of Materials Science Materials in Electronics, 2018, 29:21157-21169.

[12] Hasnine M, Vahora N, et al. Microstructural and mechanical behavior of SnCu-Ge solder alloy subjected to high temperature storage[J]. Journal of Materials Science. Materials in Electronics,

2018, 29(11):8904-8913.

[13] Wu J, Xue S B, Wang J W, et al. Effect of Pr addition on properties and Sn whisker growth of Sn-0.3Ag-0.7Cu low-Ag solder for electronic packaging[J]. Journal of Materials Science Materials in Electronics, 2017, 28(14):10230-10244.

[14] Hou Z Z, Zhao X C, Liu Y, et al. Comparative study on the hourglass-like joint of electroplated Sn-base solder reinforced by adding Ag_3Sn nanoparticles and Ag micro-alloying elements[J]. Materialia, 2020, 9:100558.

[15] Zhang Y, Lu C J, Liu Y S, et al. The effect of Bi addition on the formation of metal whiskers in Ti_2SnC/Sn-xBi system[J]. Vacuum, 2020, 182:109764.

[16] He H, Huang S Y, Xiao Y, et al. Diffusion reaction-induced microstructure and strength evolution of Cu joints bonded with Sn-based solder containing Ni-foam[J]. Materials Letters, 2020, 281:128642.

[17] Xu K K , Zhang L , Jiang N . Effect of CNTs on the intermetallic compound growth between Sn solder and Cu substrate during aging and reflowing[J]. Journal of Materials Science: Materials in Electronics, 2021, 32:2655-2666.

[18] Sun L, Chen M H, Zhang L, et al. Effect of addition of CuZnAl particle on the properties of Sn solder joint[J]. Journal of Materials Processing Technology, 2019, 278:116507.

[19] Zhao M, Zhang L, Sun L, et al. Effects of nanoparticles on properties and interface reaction of Sn solder for microelectronic packaging[J]. International Journal of Modern Physics B, 2020, 34(8): 2050064.

[20] Lee C W , Shin Y S , Yoo S H . Effect of SiC nanoparticles dispersion on the microstructure and mechanical properties of electroplated Sn-Bi solder alloy[J]. Journal of Nano Research, 2010, 11:113-118.

Figures

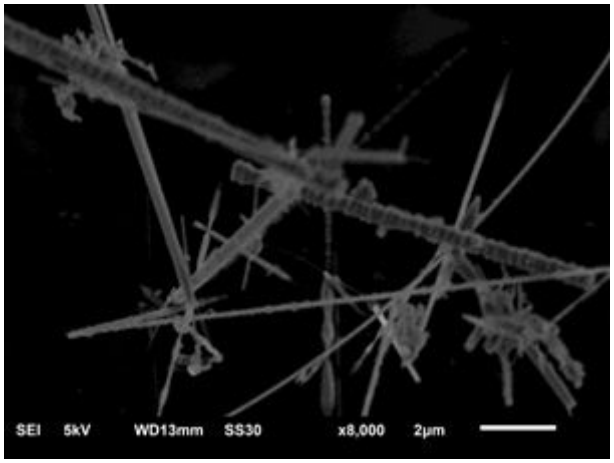

Figure 1

SEM image of SiC.

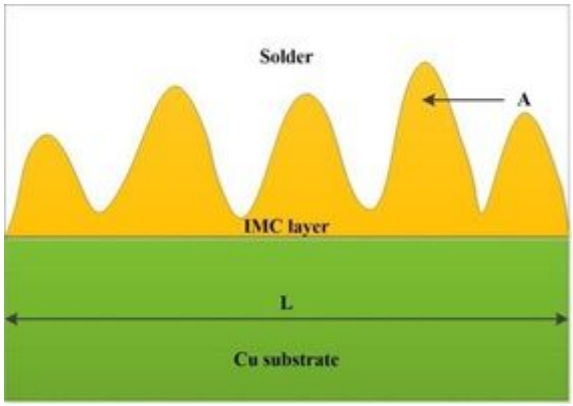

Figure 2

Diagrammatic drawing of interfacial IMC.

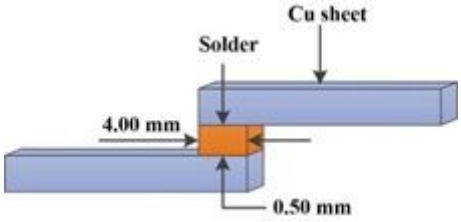

Figure 3

Diagrammatic drawing of shear test for Sn-xSiC solder.

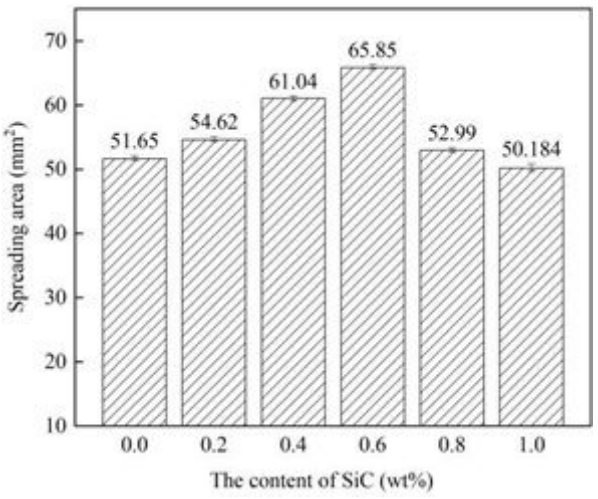

Figure 4

Column diagram of the spreading area varying with the addition content of SiC.

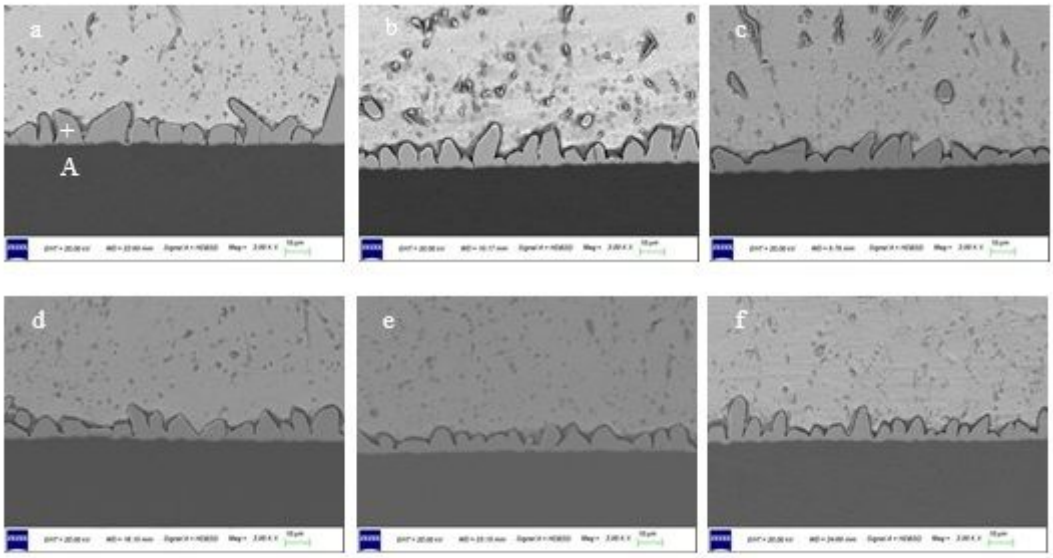

Figure 5

SEM morphology graph of the IMC at Sn-xSiC/Cu solder heated at 250 °C for 1 min: (a) x=0, (b) x=0.2, (c) x=0.4, (d) x=0.6, (e) x=0.8, (f) x=1.0.

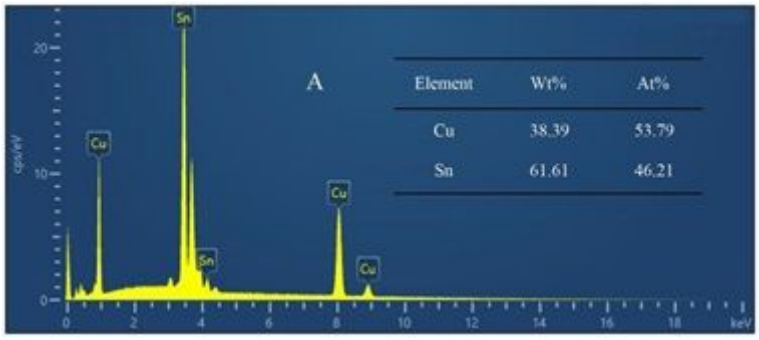

Figure 6

EDS analysis of IMC layer in Fig.4(a)

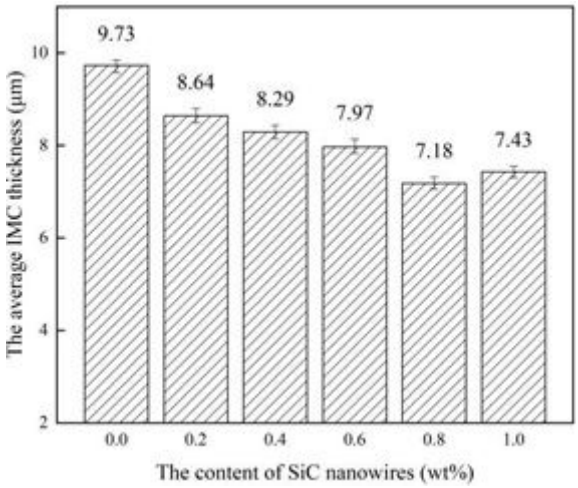

Figure 7

The average IMC thickness as different amount of SiC added to Sn solder.

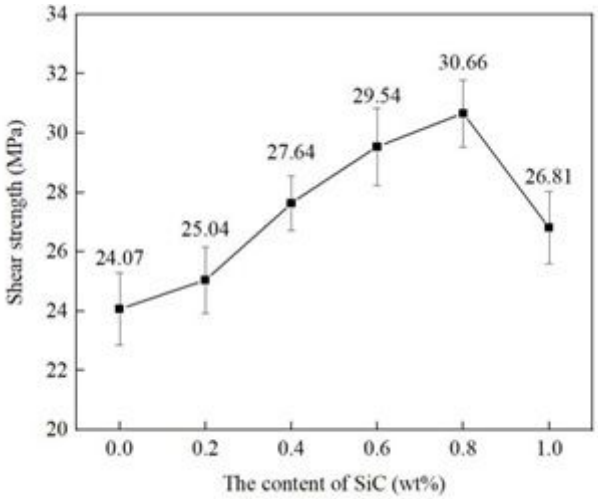

Figure 8

Curve graph of the shear strength as a function of SiC amount in Sn solder.

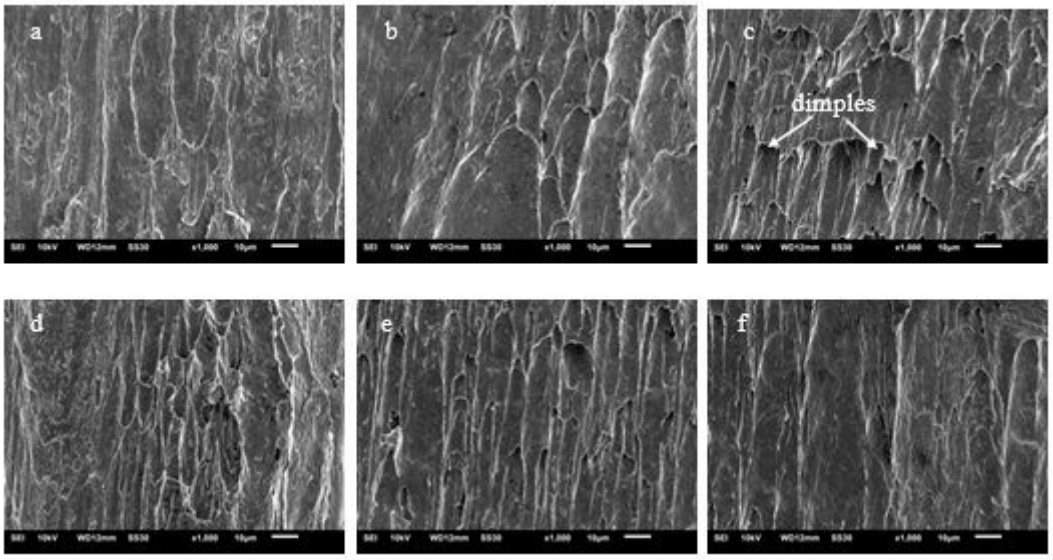

Figure 9

SEM graphs of fracture morphology of Sn-xSiC solder under tensile test: (a) x = 0, (b) x = 0.2, (c) x = 0.4, (d) x = 0.6, (e) x = 0.8, (f) x = 1.0.